Circularly symmetric watermark embedding in 2-D DFT domain

V. Solachidis and I.Pitas

Department of Informatics, University of Thessaloniki

Thessaloniki 54006, Greece Tel,Fax: +3031-996304

e-mail: pitas@zeus.csd.auth.gr

EDICS number: *5-AUTH*

Abstract

In this paper a method for digital image watermarking is described that is resistant to geometric transformations. A private key, which allows a very large number of watermarks, determines the watermark, which is embedded on a ring in the DFT domain. The watermark possesses circular symmetry. Correlation is used for watermark detection. The original image is not required in detection. The proposed method is resistant to JPEG compression, filtering, noise addition, scaling, translation, cropping, rotation, printing and rescanning. Experimental results prove the robustness of this method against the above-mentioned attacks.

I. INTRODUCTION

The development of the digital services created new requirements for multimedia security and copyright protection techniques. The copying and reproduction of digital images and their distribution through World Wide Web made the watermark protection an essential requirement for image distribution. Thus, watermarking research has been developed rapidly in the last years. The watermark is a signal that contains information about the copyright owner. It is embedded permanently in an image and introduces invisible changes for the human vision that can be detected only by a computer program.

The watermarks must be robust to distortions such as those caused by image processing algorithms. Image processing does not modify only the image but may also modify the watermark as well. Thus, the watermark may become undetectable after intentional or unintentional image processing attacks. The watermark must also be invisible. The watermark alterations should not decrease the image quality. A general watermarking framework for copyright protection has been presented in [1], [2] and describes all these issues in detail. The watermark is embedded using the Discrete Cosine Transform (DCT) [3]-[8], Discrete Fourier Transform (DFT) phase and magnitude [9],[10], wavelets [11],[12], chaos and fractals [13],[14], or can be embedded in the spatial domain [15]-[17]. There are methods that use perceptual masking in order to decrease the watermark visibility [18]-[20] and methods that decrease the watermark strength or destroy it through image manipulations [21], [22]. Watermark embedding in the Fourier domain has certain advantages for scaling and rotation invariance. The Fourier-Mellin transform has been used for watermark embedding [9],[10]. In the technique proposed in this paper we also embed watermark in the Fourier domain. However, we avoid employing the Fourier-Mellin transform in order to decrease computational complexity and to avoid the problems involved in log-polar coordinate system transformation errors. Furthermore, we use circularly symmetric watermarks in order to solve rotation invariance in an easy way.

This paper is organized as follows. The watermark design and embedding algorithm is described in the section II. The detection algorithm is presented in the third section. The robustness of the algorithm against geometrical distortions is explained in section 4. The number of different watermarks that can be produced is calculated in section 5. The algorithm complexity is examined in section 6. In the last section experimental results are shown, which depict the efficiency and the robustness of this algorithm against several distortions.

II. Watermark embedding

Let $i(n_1, n_2)$ be a $N \times N$ grayscale original image. Its discrete Fourier transform is given by:

$$I(k_1, k_2) = \sum_{n_1=0}^{N_1-1} \sum_{n_2=0}^{N_2-1} i(n_1, n_2) e^{-j2\pi n_1 k_1/N_1 - j2\pi n_2 k_2/N_2} \tag{1}$$

Let also $M(k_1, k_2) = |I(k_1, k_2)|$ be the magnitude and $P(k_1, k_2)$ the phase of $I(k_1, k_2)$ and $W(k_1, k_2)$ be the watermark. Circular shifts in the spatial domain do not effect the magnitude of Fourier transform:

$$|DFT[i(n_1 + d_1, n_2 + d_2)]| = M(k_1, k_2) \tag{2}$$

Scaling in the spatial domain causes inverse scaling in the frequency domain:

$$DFT[i(sn_1, sn_2)] = \frac{1}{s} I(\frac{k_1}{s}, \frac{k_2}{s}) \tag{3}$$

where s is the scaling factor.

Rotation in the spatial domain causes the same rotation in the frequency domain:

$$DFT[i(n_1 \cos\theta - n_2 \sin\theta, n_1 \sin\theta + n_2 \cos\theta)] = I(k_1 \cos\theta - k_2 \sin\theta, k_1 \sin\theta + k_2 \cos\theta) \quad (4)$$

The watermark is embedded in the DFT transform. It consists of 2-D sequence that takes values 1 or -1. The number of $1s$ is the same with the number of $-1s$, so that the watermark sequence has zero mean value. Modifications in the low frequencies of the Fourier transform will cause visible changes in the spatial domain. Compression affects the high frequencies of the Fourier transform. Thus, the watermark should be added in the middle frequency range because, if carefully designed, it will be robust against compression and invisible at the same time. Considering that the zero frequency term $I(0,0)$ is in the center of the transform domain, the watermark should be embedded in a ring that covers the middle frequencies:

$$W(r,\theta) = \begin{cases} 0, & \text{if } r < R_1 \text{ and } r > R_2 \\ \pm 1, & \text{if } R_1 < r < R_2 \end{cases} \quad (5)$$

where $r = \sqrt{k_1^2 + k_2^2}$, $\theta = \arctan(\frac{k_2}{k_1})$. The ring is separated in $R_2 - R_1$ homocentric circles of radius $r \in [R_1, R_2]$ and in S sectors. In each sector the value of the watermark is the same (1 or -1) as can be seen in Figure 1. Thus:

$$W(r,\theta) = x(r - R_1, \lfloor \frac{\theta S}{2\pi} \rfloor) \quad (6)$$

where $\lfloor x \rfloor$ is the biggest integer that is smaller than x. We choose circular symmetry for watermark robustness against rotation, as will be described later on. Let $M^{'}(k_1,k_2)$ be the modified magnitude and $I^{'}(k_1,k_2)$ be the watermarked image. Then the coefficients of $M^{'}(k_1,k_2)$ are:

$$M^{'}(k_1,k_2) = M(k_1,k_2) + f(M(k_1,k_2), W(k_1,k_2), a) \quad (7)$$

where a is a factor that determines the watermark strength.

The embedding function $f(M(k_1,k_2), W(k_1,k_2), a)$ can be additive or image dependent. In the case of additive watermark the embedding function has the form $f(M,W,a) = aW(k_1,k_2)$.

The simplest form of image dependent embedding is the multiplicative one $f(M,W,a) = aM(k_1,k_2)W(k_1,k_2)$. The IDFT of a real image has the complex conjugate property. In order to ensure that the IDFT of the watermarked magnitude $M^{'}(k_1,k_2)$ is real, the watermark must preserve the following symmetry [9]:

$$W(k_1,k_2) = W(N-k_1,N-k_2),\ \ \forall\, k_1,k_2 \in [1,N] \tag{8}$$

The watermarked image $i^{'}(n_1,n_2)$ is the inverse Fourier transform of $M^{'}(k_1,k_2)$ and $P(k_1,k_2)$:

$$i^{'} = IDFT(I^{'}),\ \ I^{'} = (M^{'},P) \tag{9}$$

The values of $i^{'}(n_1,n_2)$ are truncated in the region $[0,255]$. In order to increase the watermark invisibility a local image masking can be used. A masking method is based on the variance of the neighborhood of each pixel. Each pixel of the masked image is chosen from the original or the watermark image accordingly to the local variance. Similar masking methods have been presented in [19].

The original image Lenna and its watermarked version is shown in Figures 1 a,b respectively. We have used $a = 0.3$. As can be seen, the watermark is invisible. The watermark embedding in the frequency domain is shown in Figure 2. In this figure we use a large factor a for illustrative purposes.

III. Watermark detection

Let $I^{'}$ be the DFT of a possibly watermarked image and $M^{'}$ its magnitude. The correlation c between the possibly watermarked coefficients $M^{'}$ and the watermark W can be used to detect the presence of the watermark:

$$c = \sum_{k_1=1}^{N}\sum_{k_2=1}^{N} W(k_1,k_2)M^{'}(k_1,k_2) \tag{10}$$

If the image $I^{'}$ is watermarked with $W^{'}$, $W \neq W^{'}$, then the correlation c is given by:

$$c = \sum_{k_1=1}^{N}\sum_{k_2=1}^{N} (W(k_1,k_2)M(k_1,k_2) + aW(k_1,k_2)W^{'}(k_1,k_2)) \tag{11}$$

in case of additive embedding or:

$$c = \sum_{k_1=1}^{N} \sum_{k_2=1}^{N} (W(k_1,k_2)M(k_1,k_2) + aW(k_1,k_2)W^{'}(k_1,k_2)M(k_1,k_2)) \tag{12}$$

in case of multiplicative embedding.

If the image $I^{'}$ is watermarked with W, the correlation c is the following:

$$c = \sum_{k_1=1}^{N} \sum_{k_2=1}^{N} (W(k_1,k_2)M(k_1,k_2) + aW^2(k_1,k_2))(\text{additive embedding}) \tag{13}$$

$$c = \sum_{k_1=1}^{N} \sum_{k_2=1}^{N} (W(k_1,k_2)M(k_1,k_2) + aW^2(k_1,k_2)M(k_1,k_2))(\text{multiplicative embedding}) \tag{14}$$

Assuming that W, M are independent and identically distributed random variables, W has zero mean value and W, $W^{'}$ are orthogonal to each other, the mean value μ_c and the variance σ_c of c is given by:

$$\underbrace{\mu_c = \begin{cases} Ka & \text{if } W = W^{'} \\ 0 & \text{if } W \neq W^{'} \\ 0 & \text{if no watermark is present} \end{cases}}_{\text{additive embedding}} \qquad \underbrace{\mu_c = \begin{cases} Ka\,\mu_{M} & \text{if } W = W^{'} \\ 0 & \text{if } W \neq W^{'} \\ 0 & \text{if no watermark is present} \end{cases}}_{\text{multiplicative embedding}} \tag{15}$$

$$\underbrace{\sigma_c^2 = \begin{cases} K(\mu_{M}^2 + \sigma_{M}^2) & \text{if } W = W^{'} \\ K(\mu_{M}^2 + \sigma_{M}^2 + a^2) & \text{if } W \neq W^{'} \\ K(\mu_{M}^2 + \sigma_{M}^2) & \text{if no watermark is present} \end{cases}}_{\text{additive embedding}} \qquad \underbrace{\sigma_c^2 = \begin{cases} K[\mu_{M}^2 + \sigma_{M}^2(1+a^2)] & \text{if } W = W^{'} \\ K(\mu_{M}^2 + \sigma_{M}^2)(1+a^2) & \text{if } W \neq W^{'} \\ K[\mu_{M}^2 + \sigma_{M}^2] & \text{if no watermark is present} \end{cases}}_{\text{multiplicative embedding}} \tag{16}$$

where μ_{M} and σ_{M}^2 is the mean value and the variance of $M(k_1,k_2)$ and $K = \pi(R_2^2 - R_1^2)$. The derivations are given in the Appendix. The correlator c can also be expressed in normalized form $c_n = c/\mu_c$. The mean value μ_c depends on the magnitude of the Fourier transform of the original image $M(k_1,k_2)$ which is unknown. Instead of μ_{M} we can use $\mu_{M'}$ because:

$$\mu_{M'} = \overline{M}(k_1,k_2) + a\overline{W}(k_1,k_2)) = \overline{M}(k_1,k_2) = \mu_{M} \ (\text{additive embedding})$$

$$\mu_{M'} = \overline{M}(k_1,k_2) + a\overline{W}(k_1,k_2))\overline{M}(k_1,k_2) = \overline{M}(k_1,k_2) = \mu_{M} \ (\text{multiplicative embedding})$$

The mean value of the normalized correlator c_n should be 1 for every watermarked image when calculated for the correct watermark W. Generally, the watermarks that are produced by random generators do not have zero mean value. Thus, the correlator should be modified in order to avoid this problem. The modified correlator has the form:

$$c_n = \left(\frac{\sum\limits_{M' \in M'_+} M'(k_1,k_2)}{N_+} - \frac{\sum\limits_{M' \in M'_-} M'(k_1,k_2)}{N_-} \right) \frac{N_+ + N_-}{2f(M(k_1,k_2),a)}$$

$$= \left(\frac{\sum\limits_{M \in M_+} M(k_1,k_2) + f(M(k_1,k_2),a)}{N_+} - \frac{\sum\limits_{M \in M_-} M(k_1,k_2) - f(M(k_1,k_2),a)}{N_-} \right) \frac{1}{2\mu_{f(M(k_1,k_2),a)}}$$

$$\mu_{c_n} = (\mu_{M_+} + \mu_{f_+(M(k_1,k_2),a)} - \mu_{M_-} + \mu_{f_-(M(k_1,k_2),a)}) \frac{1}{2\mu_{f(M(k_1,k_2),a)}} = 1$$

where $M_+ = \{M(k_1,k_2) | W(k_1,k_2) = 1\}$, $M_- = \{M(k_1,k_2) | W(k_1,k_2) = -1\}$, $f_+(M(k_1,k_2),a) = \{f(M(k_1,k_2),a) | W(k_1,k_2) = 1\}$, $f_- = \{f(M(k_1,k_2),a) | W(k_1,k_2) = -1\}$ and N_+, N_- are the cardinalities of M_+ and M_- respectively. We assume that $\mu_{M_+} = \mu_{M_-} = \mu_{f_+(M(k_1,k_2),a)} = \mu_{f_-(M(k_1,k_2),a)}$.

The empirical pdf of c_n that has been obtained by watermarking the 512×512 'LENNA' with 1000 different watermarks is shown in Figure 3. The detection could be of the form:

H_0: I' is watermarked by W' if $c_n \geq T$

H_1: I' is not watermarked by W' if $c_n < T$

Considering that T is the threshold, two probabilities must be estimated. First, the false alarm probability P_{fa}, which is the probability to detect a watermark in an unmarked image. False rejection probability P_{fr} is the probability of not detecting the watermark in a marked image. We assume that the empirical pdf of c_n can be approximated by a normal distribution false alarm and false rejection can be computed using the error function $erf(x)$:

$$P_F = 1 - \frac{1}{2} erf\left(\frac{T}{\sqrt{2\sigma_c^2}}\right). \tag{17}$$

In our experiments the value of the threshold is chosen to be $T = 0.17$. In all the performed experiments c_n is always bigger than T when the image is watermarked and lower that T

when the image is not watermarked, even if the image is distorted, compressed or geometrically transformed. Thus, $P_{fa} = P_{fr} = 0$. If we fit a Gaussian distribution to the empirical pdf of c_n the resulted estimated errors are shown in Table 1. For certain attacks the estimated errors coming from Gaussian distribution fitting are extremely small (practically zero) and statistically insignificant [23]. It can be seen that, without distortion the errors are extremely low (FAR=6.2085 10^{-4}, FRR=1.0495 10^{-36}). The worst case scenario in out studies appear when we have rotation by 3 degrees (FAR=8.432 10^{-2}, FRR=8.659 10^{-2}). Even in this case the algorithm performance is very good.

IV. Robustness to geometrical transformations

A. Rotation

Rotation in the spatial domain causes rotation of the Fourier domain by the same angle as shown in (4). Since the watermark consists of S sectors having identical values, this construction of the watermark allows its detection even after an image rotation in the range $[-\frac{\pi}{S}, \frac{\pi}{S}]$ of the watermarked image. The maximum angle of rotation depends on the size (or the number) of the sectors. If a search for optimal rotation is performed that maximizes c', the detection algorithm can be robust to any rotation angle. Rotation and translation invariance are very useful because the digital copies coming from printing, and re-scanning maybe rotated and/or translated in comparison to the initial image. From a geometrical transformation point of view, rotation around an arbitrary center is equivalent to rotation around the center of the image and translation. Thus, our method is robust to rotation around an arbitrary center.

B. Scaling

Scaling in the spatial domain causes inverse scaling in the frequency domain (3). If $N \times M$ is the size of the initial image and $[R_1, R_2]$ is the size of the watermark ring (in the frequency domain), the size of the scaled image is (scale factor s), $sN \times sM (s > 0)$ and the size of the watermark of the scaled image in the frequency domain remains unaltered. Therefore, R_1 and

R_2 are absolute values. Thus, the mean value of the correlation c between the watermark and the ring of any scaled image whose dimensions are R_1 and R_2 is $\pi(R_2^2 - R_1^2)a$. Furthermore, normalized correlation output does not depend on the scale factor s.

C. Cropping

Cropping changes the frequency sampling step. If the size of the initial image is known, then the correlation can be done between the DFT of cropped image and the watermark, which should be changed to the same frequency sampling step of the cropped image. If the size of the initial image is not known then the correlation should be done for many frequency sampling steps by searching the maximal detector output. Let $I^{'}$ be an $M^{'} \times N^{'}$ image which is possibly scaled and cropped. The detection algorithm is applied to the watermark and to a ring of the frequency domain of $I^{'}$ whose size is bR_1 (inside radius) and bR_2 (outside radius) for every b $(0 < b < 1)$. The normalized correlation $c^{'}$ is shown in Figure 4 for several frequency sampling steps. The initial image was cropped from 512×512 to 400×400 and scaled to 512×512. We get a maximum $c^{'}$ for $b = 50 = \frac{400}{512}64$ that manifests the existence of the watermark (in this experiment $R_1 = 64$ on the 512×512 LENNA).

The proposed method is also robust to anisotropic cropping and scaling distortions. We cropped the watermarked Lenna to 512×505 pixels and rescaled it to size 512×512 pixels. The pdf of $c^{'}$ for 100 non-watermark images (left) and 100 watermarked (right) is shown in Figure 5. If we use threshold $T = 0.17$ the method is robust to such attacks.

V. Algorithmic considerations

The sample number (length) of the 2-D watermark sequence W is:

$$L = (R_2 - R_1)\frac{S}{2}$$

where $R_2 - R_1$ is the number of the homocentric circles of the ring, S is the number of the sectors. This product is divided by 2, because the watermark preserves complex conjugate symmetry. In our experiments images, the length L of the watermark sequence is $L = 2304$ for

512×512. The number of the L-length sequences is 2^L and the number of L-length sequences with mean value 0 is $\binom{L}{L/2} = \frac{L!}{(L/2)!\,(L-L/2)!}$. The number of the watermarks for $L = 2304$ is:

$$\binom{2304}{1152} = 10^{691.7938} = 6.22\ 10^{691}$$

For every watermark there might exist other non-orthogonal watermarks that can produce a false positive detector output. In order to avoid this problem, a set of watermark sequences should be constructed such that their correlation is small. Such sequences (GMW, Gold, Kasami) can be found in the literature [24]-[28].

If the watermarked image is (geometrically) unaltered or scaled the detection algorithm requires the calculation a DFT and a correlation with the watermark. If we should search for cropping (and scaling) we should perform search for several frequency sampling steps. The number of the sampling steps depends on the minimum size of the cropped image that we want to search. For example, if we want to search from size $N \times N$ to $N/k \times N/k$ we should search from $b = 1$ to $b = \frac{1}{k}$. If the search step is 4, the total number of searches is $\frac{512-512/2}{4} + 1 = 65$.

If we should search for rotation (and scaling) we should perform search for several rotations. If the sector angle is θ the watermark can be detected after rotation $\pm\frac{\theta}{3}$. For example in the experiments we use $\theta = 9°$ and the watermark can be detected for rotation angles $\pm 1°, \pm 2°, \pm 3°$ as can be seen in section IV.E. The number of the rotation searches is $\frac{360}{4\frac{\theta}{3}} = 30$, because the watermark is symmetric (we have to search only from 0 to $180 - \frac{\theta}{3}$ degrees).

If we want to search for rotation, cropping and scaling the correlation should be calculated $\frac{270}{\theta}(\frac{M-M/k}{4} + 1)$ times, where $M \times M$ is the initial size of the watermark. The advantage of the proposed method is that if we want to search only for scaling or for cropping or for some rotations only (e.g. for multiples of $\pi/2$ or $\pi/4$) the calculation is very fast.

VI. Simulation results

The proposed watermarking method was tested in a variety of images. We used many images having different frequency content (e.g. Baboon, peppers, Lenna). The original and the watermarked images of Lenna are shown in Figures 1a, 1c respectively. The PSNR of the watermarked image (after masking) is 42 db. The watermarked image of Lenna without masking is presented in Figure 1d. The histogram equalized difference between the original image a and the watermarked image with masking c is shown in Figure 1e. The histogram equalized difference between the original image a and the watermarked image without masking d is shown in Figure 1f. We have chosen $a = 0.3$, $R_1 = 51, R_2 = 165$ for the embedding procedure. The embedding algorithm that is used is image dependent. The sector angle is 9 degrees. The resistance of our method to several attacks has been studied as follows The detection was applied to 10 images for 100 different keys. The correct key was used for the detection of the watermarked images. Then the mean value and the standard deviation of the normalized correlator were calculated and the empirical pdf was plotted. We have chosen threshold $T = 0.17$. The false alarm and the false detection were calculated and are presented in Table I. In Figure 6 the ROC curves (P_{fa} versus P_{fr} probability for several thresholds) for all the studied distortions are shown in a log-log plot. It is seen that rotation causes the worst detection performance.

A. JPEG compression

The watermark embedding does not affect the high frequencies and is expected to be robust against JPEG compression. Figure 7 shows the empirical pdf of the normalized correlator for 100 compressed non-watermarked images and 100 compressed watermarked images. Figures 7a,b correspond to compression ratios 20:1 and 25.6 : 1 respectively or equivalently to quality factors 25 and 15. For compression ratio 20 : 1, P_{fa} is 8.265 10^{-11} and P_{fr} is 2.412 10^{-3}. For compression ratio 25.6 : 1, P_{fa} is 4.562 10^{-6} and P_{fr} is 3.457 10^{-3}. A compressed image is shown in Figure 8a for compression ratio 25.6 : 1. The normalized correlator output for various compression ratios is shown in Figure 8b. It is clear that the correlator output drops almost linearly with compression ratio.

B. Median and moving average filtering

A filtered watermarked image which has been filtered by a 3×3 median filter is shown in Figure 9a. The pdf of the correlator of 100 non-watermarked and 100 watermarked images that have been filtered is shown in Figure 9b . P_{fa} is 0.0024 and P_{fr} is 1.029 10^{-10}.

Figure 10a shows the watermarked image after a 3×3 moving average filtering. The pdf of the normalized correlator is shown in Figure 10b. P_{fa} is 0.009 and P_{fr} is 2.379 10^{-11}. Thus, the proposed watermarking method is expected to be robust to lowpass filtering.

C. Gaussian noise addition

Gaussian noise with zero mean and $\sigma = 20$ was added to the watermarked images. Such an image in shown in Figure 11a. The pdf of the correlator of the non-watermarked and watermarked images is shown in Figure 11b. In this case, P_{fa} is 4.3579 10^{-10} and P_{fr} is 1.5332 10^{-6}. Thus, our method is resistant to additive Gaussian noise corruption.

D. Cropping

A cropped and watermarked 256×256 Lenna is shown in Figure 12a. The empirical pdf of the normalized correlator is shown in Figure 12b. P_{fa} is 2.342 10^{-3} and P_{fa} is 4.376 10^{-6}. Thus, the proposed method is very resistant to cropping.

E. Rotation

The watermark is circularly symmetric in order to be resistant to small rotations. The watermarked image, which has been rotated by 1 degree is shown in Figure 13a. The pdf of the correlator of the rotated non-watermarked image and watermarked image is shown in Figure 13b. P_{fa} is 5.4487 10^{-8} and P_{fr} is 7.2221 10^{-16}. For a rotation of 2 degrees (Figure 14), P_{fa} is 4.327 10^{-3} and P_{fr} is 4.981 10^{-8}. For a rotation of 3 degrees (Figure 15), P_{fa} is 8.432 10^{-2} and P_{fr} is 8.65910^{-2}. The watermarked image which has been rotated 90 degrees is shown in Figure 16a. In order to detect a watermark in a possibly rotated image, the DFT of the watermarked image is correlated with the watermark, which is rotated for several angles. The correlation output for several angles and frequency sampling steps is shown in Figure 16b. The maximal correlator output is 0.3474, which is above the threshold and gives correct positive detection output. Furthermore, the search for several several frequency sampling steps and rotations does not increase the false alarm probability. Experiments shows that $P_{fa} = 7.6410^{-4}$.

F. Anti-watermarking systems

This method was also tested with two programs that have been designed to test or remove watermarks. The first one is StirMark (version 2) [21]. In our experiment we used the default distortion parameters. Some of the distortions used by StirMark are filtering, JPEG compression, cropping and scaling. The output of the StirMark software is shown in Figure 17a. The normalized correlator for several frequency sampling steps is shown in Figure 17b. The image is cropped, thus the detector output has to be calculated for different sampling steps. The maximal correlator output is 0.295427 which shows that the watermark was detected successfully. The PSNR of the output image is 20.94.

Another anti-watermarking system tested is the UnZign software. Some of the distortions caused by UnZign is compression and cropping. The compression ratio is 8.25 : 1 and the size of the result image is cropped to 509×512 from 512×512 (Figure 18a). In this case the watermark was also detected, since the maximal correlator value is 0.591259 (Figure 18b). The PSNR of the output image is 28.62.

G. Printing and scanning

The watermarked image, which is the result of printing and re-scanning, is shown in Figure 19. The scanning was not so accurate, so the scanned image had to be cropped in some parts. The maximal correlator output was 0.3684 (Figure 19b) and the watermark was correctly detected. In Figure 20a the watermarked image was slightly rotated when it was re-scanned and the scanned image was cropped in order to remove the background. The Moire patterns are evident due to dithering and rotation before rescanning. In this case, the maximal correlator value 0.3068 is above detection threshold (Figure 20b).

H. Grayscale quantization

The watermarked images that have been produced after image quantization are shown in Figures 21a, 22a, 23a. The empirical pdf of the normalized correlator of 100 non watermarked color quantized images (left) and 100 watermarked color quantized images (right) are shown in Figures 21b, 22b, 23b. P_{fa} is 0.001, 2.473 10^{-5}, 9.6557 10^{-4} and P_{fr} is 5.1917 10^{-14}, 1.0808 10^{-4}, 5.3478 10^{-24} respectively.

I. Other distortions

The negative watermarked image is shown in Figure 24a. The frequency content of the watermarked image is the similar with the inverse watermarked image in the frequency domain where the watermark is embedded. In this case P_{fa} is 6.2085 10^{-4} and P_{fr} is 2.4469 10^{-48}.

A watermarked image is shown in Figure 25 that has been produced after histogram equalization. P_{fa} is 4.0111 10^{-4} and P_{fr} is 6.4438 10^{-53}.

Figure 26a shows a watermarked image which was compressed (compression ratio 1 : 14.22), rotated (30 degrees), cropped to 400×400, scaled to 512×512 and histogram equalized. The correlator output for several sampling steps and rotations is shown in Figure 26b. The maximal correlator output is 0.2914. This experiment illustrates that the watermark is robust to combined attacks.

VII. Conclusions

In this paper we present a watermarking method based on circularly symmetric watermarks applied in the DFT domain. In this method the original image is not required in the detection procedure. A circularly symmetric watermark is added in the middle frequencies of the DFT image domain. This method is robust to several image processing attacks such as filtering, noise addition, scaling, rotation, cropping, JPEG compression. In all the experiments performed the detector output c_n was always bigger than the chosen threshold T in the case of a watermarked image and smaller than T in the case of a non-watermarked image, leading to practically zero errors.

Using the translation invariance property of DFT we can detect a watermark in a scaled and cropped watermarked image just by correlating the watermark and the magnitude of the DFT of the image for several frequency sampling steps. Also, due to rotation property and the division of the watermark domain in sectors, the watermark is detectable after a small rotation (up to 3 degrees). Correlation with rotated watermarks for several angles can detect a watermark for any rotation angle of the watermarked image.

References

[1] G. Voyatzis and I. Pitas. Protecting digital-image copyrights: A framework. *IEEE Computer Graphics and Applications*, 19(1):18–24, January/February 1999.

[2] G.Voyatzis and I.Pitas. The use of watermark in the rotection of digital multimedia products. *IEEE Proceedings Special issue on Identification and protection of multimedia information*, to appear July 1999.

[3] M. D. Swanson, B. Zhu, and A. H. Tewfik. Transparent robust image watermarking. In *Proceedings of ICIP'96*, volume III, pages 211–214, Lausanne, Switzerland, September 1996.

[4] I. J. Cox, J. Kilian, F. T. Leighton, and T. Shamoon. Secure spread spectrum watermarking for multimedia. *IEEE Transactions on Image Processing*, 6(12):1673–1687, 12 1997.

[5] A.G. Bors and I. Pitas. Image watermarking using dct domain constraints. In *Proc. of ICIP'96*, volume III, pages 231–234, Lausanne, Switzerland, September 1996.

[6] A. Piva, M.Barni, and F. Bartolini. DCT-based watermark recovering without resorting to the uncorrupted original image. In *Proc. of ICIP'97*, volume I, pages 520–523, Atlanta, USA, October 1997.

[7] M.Barni, F.Bartolini, V.Cappelini, and A.Piva. A blind dct-domain system for robust image watermarking. *to appear in IEEE Journal of Selected Areas of Communications.*

[8] C.T. Hsu and J.L. Wu. Hidden signatures in images. In *Proc. of ICIP'96*, volume III, pages 223–226, Lausanne, Switzerland, September 1996.

[9] J. Ó Ruanaidh, W.J. Dowling, and F.M. Boland. Phase watermarking of digital images. In *Proc. of ICIP'96*, volume III, pages 239–242, Lausanne, Switzerland, September 1996.

[10] J. Ó Ruanaidh and T. Pun. Rotation, scale and translation invariant digital image watermarking. In *Proc. of ICIP'97*, volume I, pages 536–539, Atlanta, USA, October 1997.

[11] H. Inoue, A. Miyazaki, A. Yamamoto, and T. Katsura. A digital watermark based on wavelet transform and its robustness on image compression. In *Proc. of ICIP'98*, volume II, pages 391–395, Chicago, Illinois, USA, 4-7 October 1998.

[12] R. Dugad, H. Ratakonda, and N. Ahuja. A new wavelet-based scheme for watermarking images. In *Proc. of ICIP'98*, volume II, pages 419–423, Chicago, Illinois, USA, 4-7 October 1998.

[13] P. Bas, J.-M. Chassery, and F. Davoine. Using the fractal code to watermark images. In *Proc. of ICIP'98*, volume I, pages 469–473, Chicago, Illinois, USA, 4-7 October 1998.

[14] G.Voyatzis and I.Pitas. Chaotic watermarks for embedding in the spatial digital image domain. In *Proc. of ICIP'98*, volume II, pages 432–436, Chicago, USA, 4-7 October 1998.

[15] Martin Kutter, Frederic Jordan, and Frank Bossen. Digital watermarking of color images using amplitude modulation. *Journal of Electronic Imaging*, 7(2):326–332, 1998.

[16] G. Voyatzis and I. Pitas. Embedding robust watermarks by chaotic mixing. In *Proceedings of 13th International Conference on Digital Signal Processing*, volume 1, pages 213–216, Santorini, Greece, July 2-4 1997.

[17] N. Nikolaidis and I. Pitas. Robust image watermarking in the spatial domain. *Signal Processing, sp.issue on Copyright Protection and Access control*, 66(3):385–403, May 1998.

[18] M.D. Swanson, B. Zhu, and A.H. Tewfik. Multiresolution scene-based video watermarking using perceptual models. *IEEE Journal of Selected Areas of Communications*, 16(4):540–550, May 1998.

[19] F.Bartolini, M.Barni, V.Cappelini, and A.Piva. Mask building for perceptually hiding frequency embedded watermarks. In *Proc. of ICIP'98*, volume I, pages 450–454, Chicago, USA, 4-7 October 1998.

[20] C.I. Podilchuk and W. Zeng. Image-adaptive watermarking using visual models. *IEEE Journal on Selected Areas in Communications*, 16(4):525–539, May 1998.

[21] A.P. Petitcolas, R.J. Anderson, and M.G. Kuhn. Attacks on copyright marking systems. In *Proc. of 2nd Information Hiding Workshop.* URL http://www.cl.cam.ac.uk/Research/Security.

[22] S. Craver, N. Memon, B-L. Yeo, and M. Yeung. Resolving rightful ownerships with invisible watermarking techniques: Limitations, attacks and implications. *IEEE Journal of Selected Areas in Communications*, 16(4), May 1998.

[23] Matt L. Miller and Jeffrey A. Bloom. Computing the probability of false watermark detection. In *Proceedings of the Third International Workshop on Information Hiding*, pages 146–158, 1999.

[24] B.Gordon, W.H.Mills, and L.R.Welch. Some new difference sets. *Canad.J.Math.*, 14:614–625, 1962.

[25] R.Gold. Optimum binary sequences for spread spectrum multiplexing. *IEEE Trans. Inform. Theory*, IT-13:619–621, October 1967.

[26] T.Kasami. Weight distribution formula for some class of cyclic codes. *Coordinated science Lab, Univ. Illinois, Urbana. Tech. Rep R-285*, April 1966.

[27] M.K.Simon, J.K.Omura, R.A.Scholtz, and B.K.Levitt. Crosscorrelation properties of pseudorandom and related sequences. *Proc. of the IEEE*, 68(5):593–619, May 1980.

[28] M.K.Simon, J.K.Omura, Scholtz R.A, and B.K.Levitt. *Spread spectrum communications handbook*. McGraw-Hill, 1994.

Appendix

I. Calculation of variance of correlator c

We assume that:

- μ_M is the mean value of $M(k_1, k_2)$ in the ring ($\mu_M = \frac{1}{\pi(R_2^2 - R_1^2)} \sum_{k_1,k_2 \in ring} M(k_1, k_2)$),
- μ_W is the mean value of the watermark,
- σ_M^2 the variance of $M(k_1, k_2)$ ($\forall k_1, k_2 \in ring$)
- σ_W^2 the variance of the watermark.
- K is the number of the values of the watermark which are not 0 (the area of the ring $K = \pi(R_2^2 - R_2^2)$). We denote this area $R = \{(x, y) \in \mathbb{N}^2 / R_1^2 \leq (x - \frac{M}{2})^2 + (y - \frac{M}{2})^2 \leq R_2^2\}$.
- $M_{\mathbf{i}} = M(i, j)$ are i.i.d. variables.
- $M_{\mathbf{i}}$ are independent from $W_{\mathbf{i}} = W(i, j)$

The possible values of the watermark are -1 and 1. Thus, the probability distribution function of the watermark and the $E(X^n)$ are:

$$f_x(x) = \begin{cases} 0.5 & , x = 1 \\ 0.5 & , x = -1 \\ 0 & , otherwise \end{cases} \qquad E(X^n) = \begin{cases} 0 & , n = 2k+1 \\ 1 & , n = 2k \end{cases} \tag{18}$$

A. Additive embedding

A.1 A watermark is present in the image

$$c = \sum_{\mathbf{i} \in \mathbf{R}} (M_{\mathbf{i}} W_{\mathbf{i}} + a W_{\mathbf{i}}^2) \tag{19}$$

$\sigma_c^2 \;\; = var(c) = E(c^2) - E^2(c) =$

$E[[\sum_{\mathbf{i} \in R} (M_{\mathbf{i}} W_{\mathbf{i}} + a W_{\mathbf{i}}^2)]^2] - E^2[\sum_{\mathbf{i} \in R} (M_{\mathbf{i}} W_{\mathbf{i}} + a W_{\mathbf{i}}^2)] \quad \mathit{(1)}$

- $[\sum_{\mathbf{i}}^{M} (Q_{\mathbf{i}})]^2 = \sum_{\mathbf{i}}^{M} Q^2 + \sum_{\mathbf{i}}^{M} \sum_{\mathbf{i} \neq \mathbf{j}}^{M} Q_{\mathbf{i}} Q_{\mathbf{j}} \quad \mathit{(2)}$
- $E[[\sum_{\mathbf{i} \in R} (M_{\mathbf{i}} W_{\mathbf{i}} + a W_{\mathbf{i}}^2)]^2] \overset{(2)}{=}$

  $E[\sum_{\mathbf{i} \in R} (M_{\mathbf{i}} W_{\mathbf{i}} + a W_{\mathbf{i}}^2)^2] + \sum_{\mathbf{i}} \sum_{\mathbf{i} \neq \mathbf{j}} [M_{\mathbf{i}} W_{\mathbf{i}} + a W_{\mathbf{i}}^2][M_{\mathbf{j}} W_{\mathbf{j}} + a W_{\mathbf{j}}^2] =$

  $K[(\mu_M^2 + \sigma_M^2)] + K^2 a^2 \quad \mathit{(3)}$
- $E^2[\sum_{\mathbf{i} \in R} (M_{\mathbf{i}} W_{\mathbf{i}} + a W_{\mathbf{i}}^2)] = [\sum_{\mathbf{i} \in R} E(M_{\mathbf{i}}) E(W_{\mathbf{i}}) + a E(W_{\mathbf{i}}^2)]^2 = a^2 K^2 \quad \mathit{(4)}$
- $\mathit{(1)(3)(4)} var(c) = K[(\mu_M^2 + \sigma_M^2)] + K^2 a^2 - a^2 K^2 = K[(\mu_M^2 + \sigma_M^2)] \qquad (20)$

A.2 A different watermark is present in the image

$$c = \sum_{\mathbf{i} \in \mathbf{R}} (M_{\mathbf{i}} W_{\mathbf{i}} + a W_{\mathbf{i}} W_{\mathbf{i}}') \tag{21}$$

$\sigma_c^2 \;\; = var(c) = E(c^2) - E^2(c) =$

$E[[\sum_{\mathbf{i} \in R} (M_{\mathbf{i}} W_{\mathbf{i}} + a W_{\mathbf{i}} W_{\mathbf{i}}')]^2] - E^2[\sum_{\mathbf{i} \in R} (M_{\mathbf{i}} W_{\mathbf{i}} + a W_{\mathbf{i}} W_{\mathbf{i}}')] \quad \mathit{(5)}$

- $E[[\sum_{\mathbf{i} \in R} (M_{\mathbf{i}} W_{\mathbf{i}} + a W_{\mathbf{i}} W_{\mathbf{i}}')]^2] \overset{(2)}{=}$

  $E[\sum_{\mathbf{i} \in R} (M_{\mathbf{i}} W_{\mathbf{i}} + a W_{\mathbf{i}} W_{\mathbf{i}}')^2] + E[\sum_{\mathbf{i}} \sum_{\mathbf{i} \neq \mathbf{j}} [M_{\mathbf{i}} W_{\mathbf{i}} + a W_{\mathbf{i}} W_{\mathbf{i}}'][M_{\mathbf{j}} W_{\mathbf{j}} + a W_{\mathbf{j}} W_{\mathbf{j}}']] =$

  $K(\mu_M^2 + \sigma_M^2 + a^2) \quad \mathit{(6)}$
- $E^2[\sum_{\mathbf{i} \in R} (W_{\mathbf{i}} + a M_{\mathbf{i}} W_{\mathbf{i}} W_{\mathbf{i}}')] = [\sum_{\mathbf{i} \in R} (E(M_{\mathbf{i}}) E(W_{\mathbf{i}}) + a E(W_{\mathbf{i}}) E(W_{\mathbf{i}}')]^2 = 0 \quad \mathit{(7)}$
- $\mathit{(5)(6)(7)} var(c) = K(\mu_M^2 + \sigma_M^2 + a^2) \qquad (22)$

A.3 No mark is present in the image

By setting $a = 0$ in (20), we have the variance of c for a non-watermarked image $K(\mu_M^2 + \sigma_M^2)$.

B. Multiplicative embedding

B.1 A watermark is present in the image

$$c = \sum_{\mathbf{i}\in\mathbf{R}} (M_\mathbf{i}W_\mathbf{i} + aM_\mathbf{i}W_\mathbf{i}^2) \quad (23)$$

$$\sigma_c^2 = var(c) = E(c^2) - E^2(c) =$$

$$E[[\sum_{\mathbf{i}\in R}(M_\mathbf{i}W_\mathbf{i} + aM_\mathbf{i}W_\mathbf{i}^2)]^2] - E^2[\sum_{\mathbf{i}\in R}(M_\mathbf{i}W_\mathbf{i} + aM_\mathbf{i}W_\mathbf{i}^2)] \quad (8)$$

- $E[[\sum_{\mathbf{i}\in R}(M_\mathbf{i}W_\mathbf{i} + aM_\mathbf{i}W_\mathbf{i}^2)]^2] \stackrel{(2)}{=}$

  $E[\sum_{\mathbf{i}\in R}(M_\mathbf{i}W_\mathbf{i} + aM_\mathbf{i}W_\mathbf{i}^2)^2] + \sum_{\mathbf{i}}\sum_{\mathbf{i}\neq\mathbf{j}}[M_\mathbf{i}W_\mathbf{i} + aM_\mathbf{i}W_\mathbf{i}^2][M_\mathbf{j}W_\mathbf{j} + aM_\mathbf{j}W_\mathbf{j}^2] =$

  $K[(\mu_M^2 + \sigma_M^2) + a^2\mu_{M^2}] + K(K-1)a^2\mu_M^2 (9)$

- $E^2[\sum_{\mathbf{i}\in R}(M_\mathbf{i}W_\mathbf{i} + aM_\mathbf{i}W_\mathbf{i}^2)] = [\sum_{\mathbf{i}\in R} E(M_\mathbf{i})E(W_\mathbf{i}) + aE(M_\mathbf{i})E(W_\mathbf{i}^2)]^2 = a^2K^2\mu_M^2 (10)$

- $(8)(9)(10) var(c) = K(\mu_M^2 + \sigma_M^2) + Ka^2(\mu_M^2 + \sigma_M^2) + K(K-1)a^2\mu_M^2 - a^2K^2\mu_M^2 =$

  $K[\mu_M^2 + \sigma_M^2 + a^2\mu_M^2 + a^2\sigma_M^2 + Ka^2\mu_M^2 - a^2\mu_M^2 - Ka^2\mu_M^2] = K[\mu_M^2 + \sigma_M^2(a^2+1)] (24)$

B.2 A different watermark is present in the image

$$c = \sum_{\mathbf{i}\in\mathbf{R}} (M_\mathbf{i}W_\mathbf{i} + aM_\mathbf{i}W_\mathbf{i}W'_\mathbf{i}) \quad (25)$$

$$\sigma_c^2 = var(c) = E(c^2) - E^2(c) =$$

$$E[[\sum_{\mathbf{i}\in R}(M_\mathbf{i}W_\mathbf{i} + aM_\mathbf{i}W_\mathbf{i}W'_\mathbf{i})]^2] - E^2[\sum_{\mathbf{i}\in R}(M_\mathbf{i}W_\mathbf{i} + aM_\mathbf{i}W_\mathbf{i}W'_\mathbf{i})] \quad (11)$$

- $E[[\sum_{\mathbf{i}\in R}(M_\mathbf{i}W_\mathbf{i} + aM_\mathbf{i}W_\mathbf{i}W'_\mathbf{i})]^2] \stackrel{(2)}{=}$

  $E[\sum_{\mathbf{i}\in R}(M_\mathbf{i}W_\mathbf{i} + aM_\mathbf{i}W_\mathbf{i}W'_\mathbf{i})^2] + E[\sum_{\mathbf{i}}\sum_{\mathbf{i}\neq\mathbf{j}}[M_\mathbf{i}W_\mathbf{i} + aM_\mathbf{i}W_\mathbf{i}W'_\mathbf{i}][M_\mathbf{j}W_\mathbf{j} + aM_\mathbf{j}W_\mathbf{j}W'_\mathbf{j}]] =$

  $K(\mu_M^2 + \sigma_M^2 + a^2\mu_{M^2}) \quad (12)$

- $E^2[\sum_{\mathbf{i}\in R}(M_\mathbf{i}W_\mathbf{i} + aM_\mathbf{i}W_\mathbf{i}W'_\mathbf{i})] = [\sum_{\mathbf{i}\in R}(E(M_\mathbf{i})E(W_\mathbf{i}) + aE(M_\mathbf{i})E(W_\mathbf{i})E(W'_\mathbf{i})]^2 = 0 \quad (13)$

- $(11)(12)(13) var(c) = K[\mu_M^2 + \sigma_M^2 + a^2(\mu_M^2 + \sigma_M^2)] = K(\mu_M^2 + \sigma_M^2)(a^2+1) \quad (26)$

B.3 No mark is present in the image

By setting $a = 0$ in (24), we have the variance of c for a non-watermarked image $K(\mu_M^2 + \sigma_M^2)$.

List of Tables

List of Figures

TABLE I

False alarm and false rejection probabilities for various distortions of the 10 watermarked images

Distortion	False alarm probability	False rejection probability
No distortion	$6.2085\,10^{-4}$	$1.0495\,10^{-36}$
Jpeg compression 1:20	$8.265\,10^{-11}$	$2.412\,10^{-3}$
Jpeg compression 1:25.6	$4.562\,10^{-6}$	$3.457\,10^{-3}$
Median filtering 3 $\times$ 3	0.0024	$1.029\,10^{-10}$
Moving average filtering 3 $\times$ 3	0.009	$2.379\,10^{-11}$
Gaussian noise addition σ=20	$4.3519\,10^{-10}$	$1.5332\,10^{-6}$
Cropping 512 $\times$ 512 $\rightarrow$ 256 $\times$ 256	$2.342\,10^{-3}$	$4.376\,10^{-6}$
Histogram equalization	$4.0111\,10^{-4}$	$6.4436\,10^{-53}$
Negative	$6.2085\,10^{-2}$	$8.2950\,10^{-33}$
Quantization to 2 bits	0.001	$2.4753\,10^{-5}$
Quantization to 3 bits	$9.6557\,10^{-4}$	$5.1917\,10^{-14}$
Quantization to 4 bits	$1.0808\,10^{-4}$	$5.3478\,10^{-24}$
Rotation 1 degree	$5.4487\,10^{-3}$	$7.2221\,10^{-16}$
Rotation 2 degrees	$4.327\,10^{-3}$	$4.981\,10^{-8}$
Rotation 3 degrees	$8.432\,10^{-2}$	$8.659\,10^{-2}$

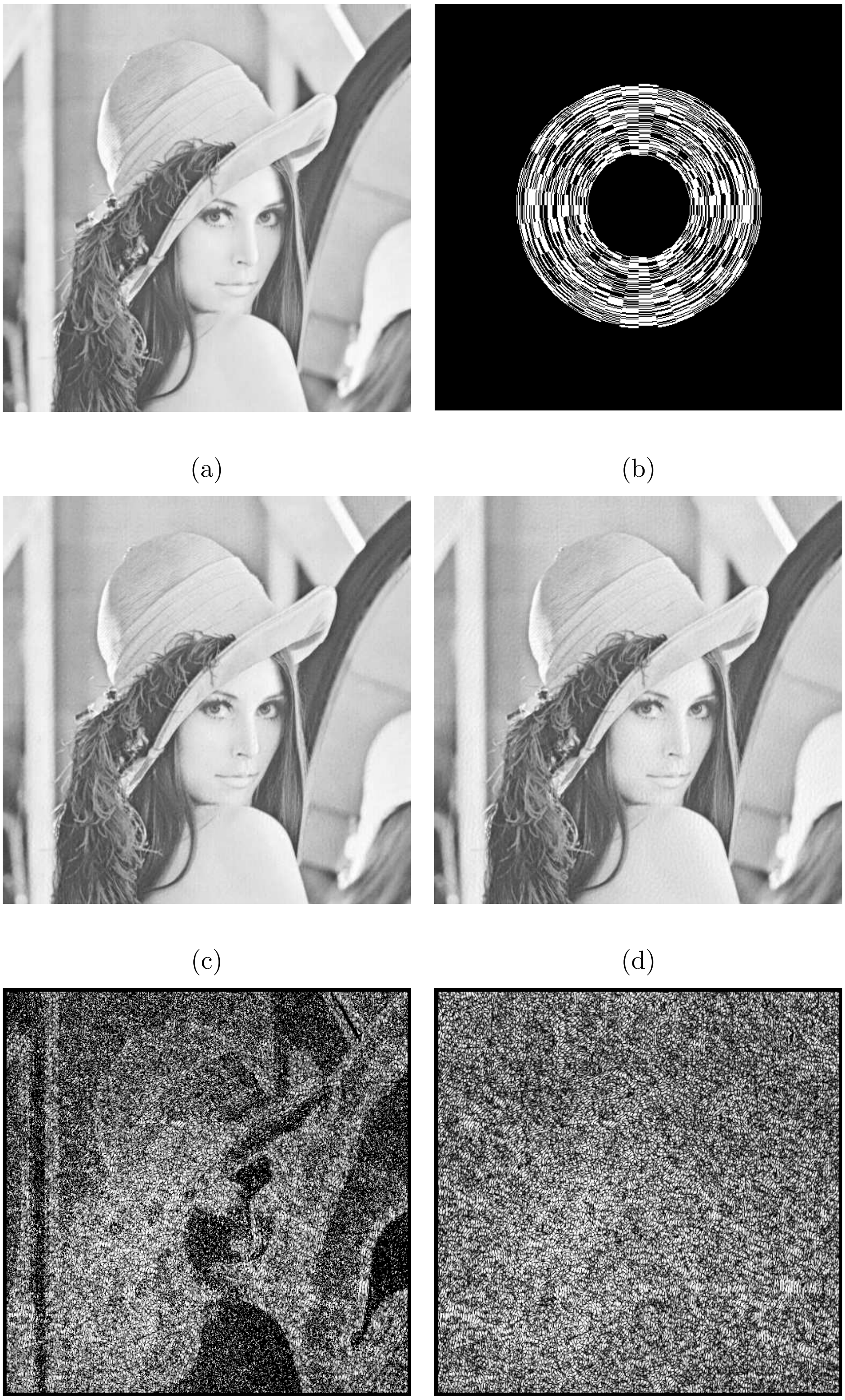

(a) (b)

(c) (d)

(e) (f)

Fig. 1. (a) Original image LENNA of size 512×512 pixels, (b)Watermark, (c) Watermarked image LENNA, (d) Watermarked image LENNA without masking, (e) Histogram equalized difference between image a and c, (f) Histogram equalized difference between image a and d.

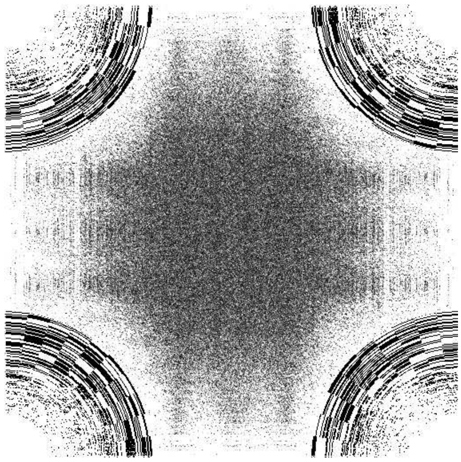

Fig. 2. Watermarked DFT magnitude of image LENNA 512×512.

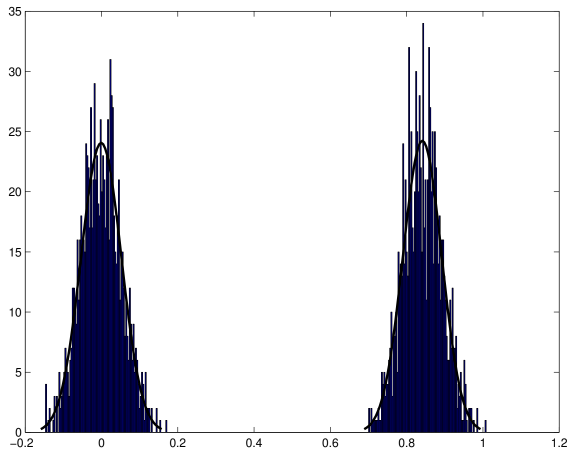

Fig. 3. Distribution of the normalized correlator output of 1000 non watermarked images (left) and 1000 watermarked images.

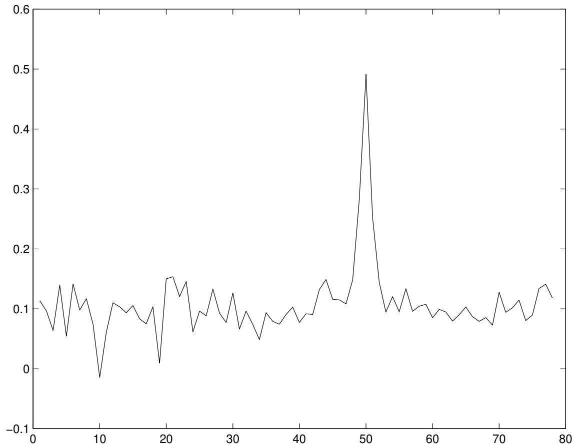

Fig. 4. Normalized correlator output for several frequency sampling steps for a cropped version of image Lenna.

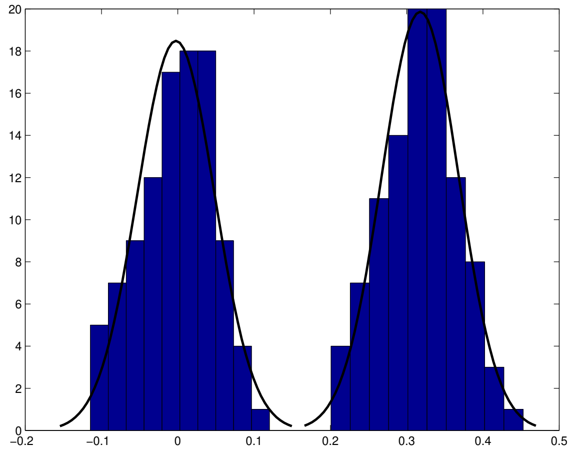

Fig. 5. Empirical pdf of the normalized correlator output of one-dimensional cropping and scaling.

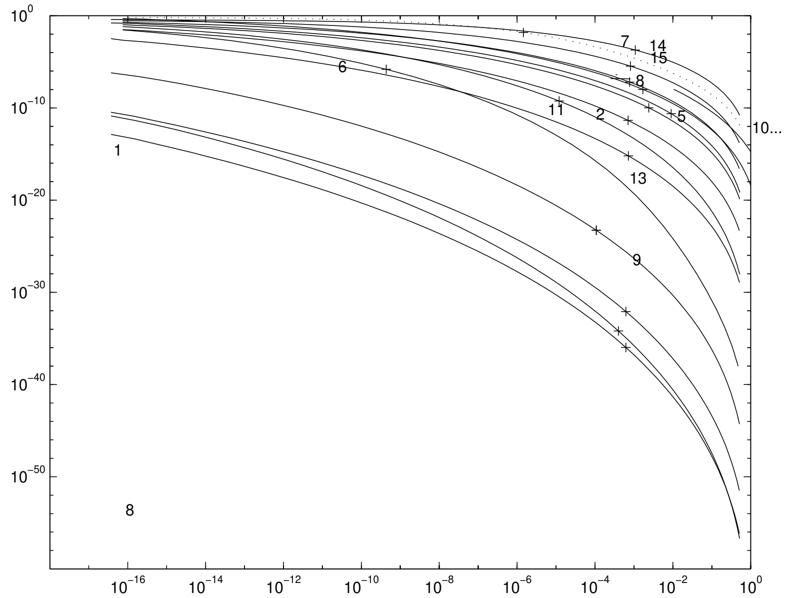

(1) No distortion
(2) Jpeg compression 1 : 20
(3) Jpeg compression 1 : 25
(4) Median filtering 3 × 3
(5) Moving average filtering 3 × 3
(2) Gaussian noise addition σ=20
(7) Cropping 512 × 512 → 256 × 256
(8) Histogram equalization
(9) Negative
(10) Quantization to 2 bits
(18) Quantization to 3 bits
(12) Quantization to 3 bits
(13) Rotation 1 degree
(14) Rotation 2 degrees
(15) Rotation 3 degrees

Fig. 6. ROC curves for each distortion (in a log-log map), where the + sign corresponds to threshold value $T = 0.17$.

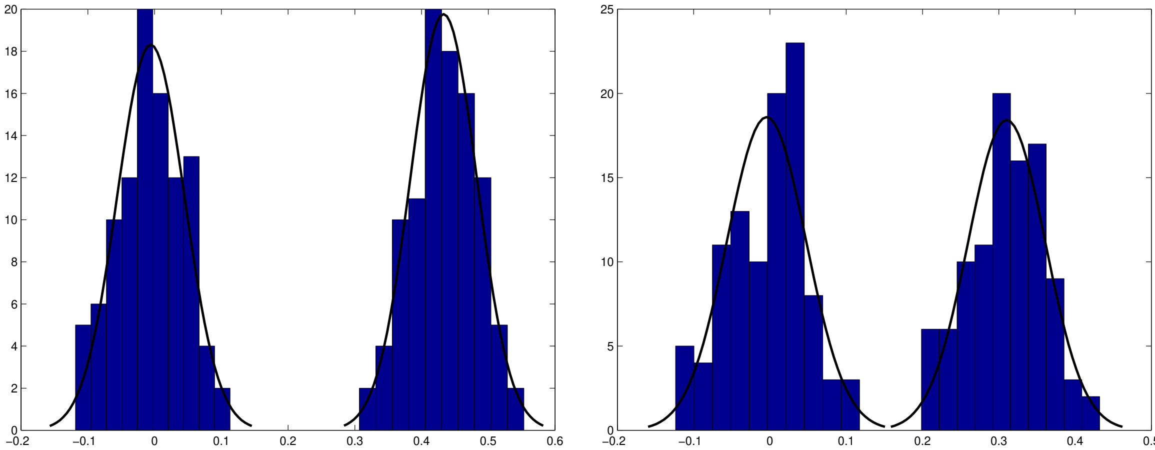

(a) (b)

Fig. 7. Empirical pdf of the normalized correlator output applied on 100 watermarked and non-watermarked JPEG compressed images (a)(compression ratio 20:1) ,(b) (compression ratio 25:1).

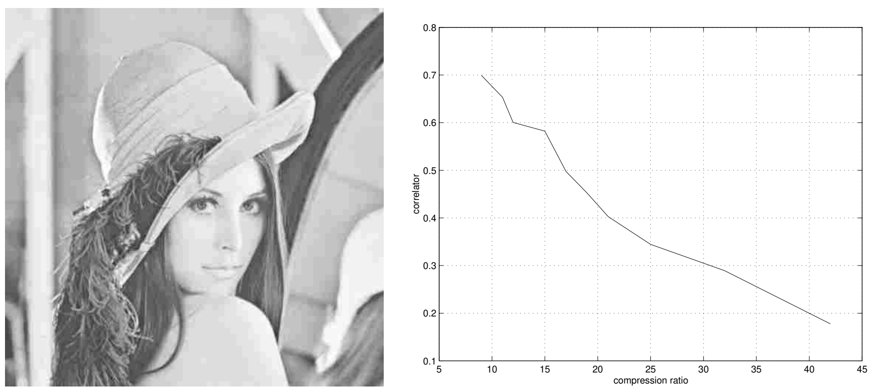

(a) (b)

Fig. 8. (a) Compressed watermarked image (Compression ratio 25.6:1), (b) Normalized correlator output for various compression ratios for watermarked Lenna 512×512.

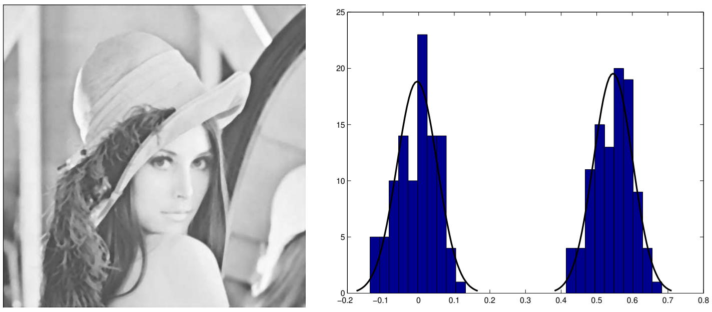

(a) (b)

Fig. 9. (a) Watermarked image filtered by median filter 3×3, (b) Empirical pdf of the normalized correlator output for 100 non-watermarked and watermarked images filtered by a 3×3 median filter.

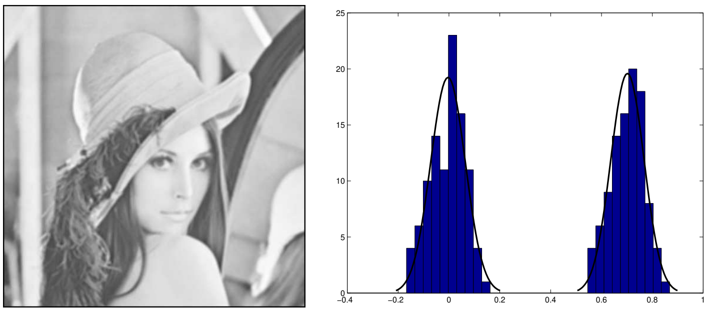

(a) (b)

Fig. 10. (a) Watermarked image filtered by a 3×3 moving average filter, (b) Empirical pdf of the normalized correlator output for 100 non-watermarked and watermarked images filtered by 3×3 moving average filter.

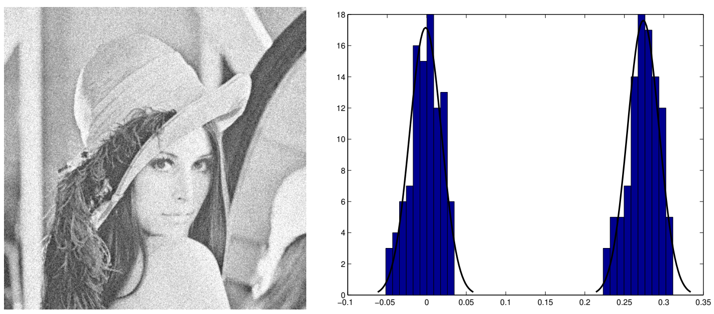

(a) (b)

Fig. 11. (a) Watermarked image corrupted by Gaussian noise having $\sigma = 20$, (b) Empirical pdf of the normalized correlator output for 100 non-watermarked and watermarked images corrupted by Gaussian noise having $\sigma = 20$.

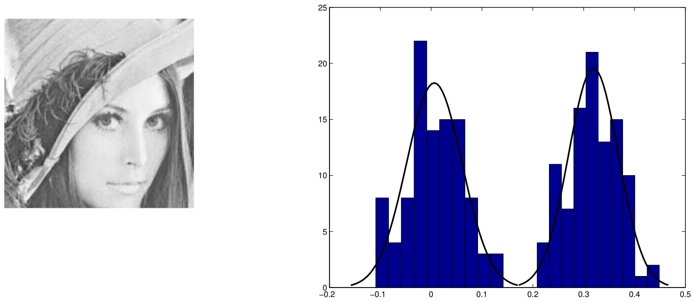

(a) (b)

Fig. 12. (a) Watermarked image cropped to size 256×256, (b) Empirical pdf of the normalized correlator output for 100 non-watermarked cropped and watermarked cropped images.

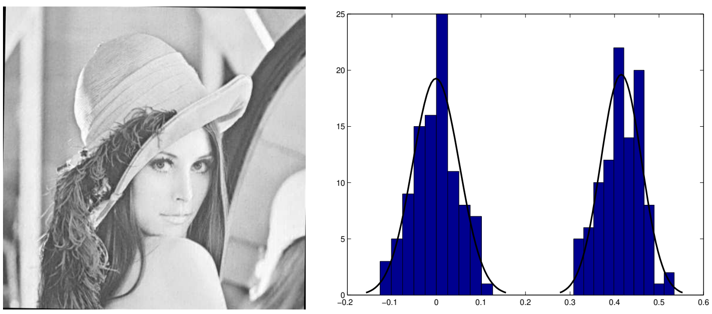

(a) (b)

Fig. 13. (a) Watermarked image after 1 degree rotation, (b) Empirical pdf of the normalized correlator output for 100 non-watermarked and watermarked cropped images (1 degree rotation).

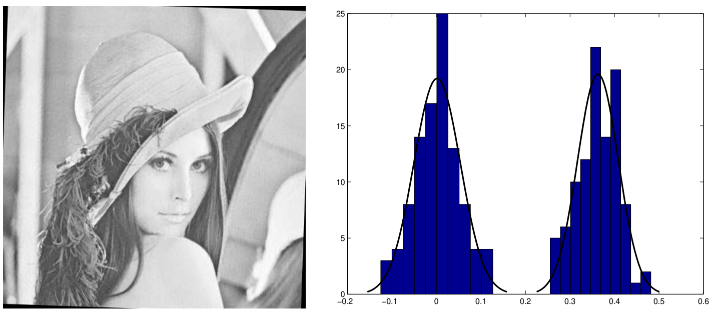

(a) (b)

Fig. 14. (a) Watermarked image after 2 degrees rotation (b) Empirical pdf of the normalized correlator output for 100 non-watermarked and watermarked cropped images (2 degrees rotation).

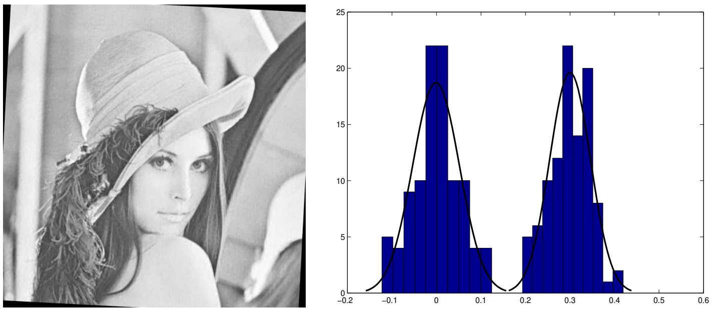

(a) (b)

Fig. 15. (a) Watermarked image after 3 degrees rotation (b) Empirical pdf of the normalized correlator output for 100 non-watermarked and watermarked cropped images (3 degrees rotation).

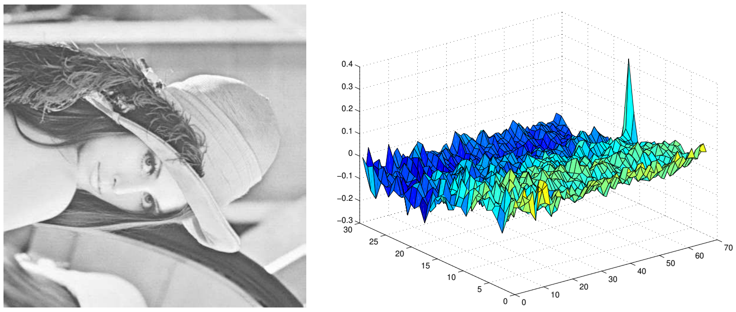

(a) (b)

Fig. 16. (a) Watermarked image rotated 90 degrees (b)Watermark detection for several sampling steps and rotations.

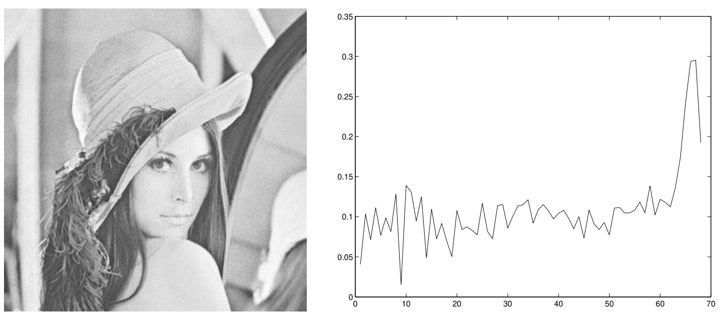

(a) (b)

Fig. 17. (a) Watermarked image after StirMark application, (b) Normalized correlator output for several frequency sampling steps.

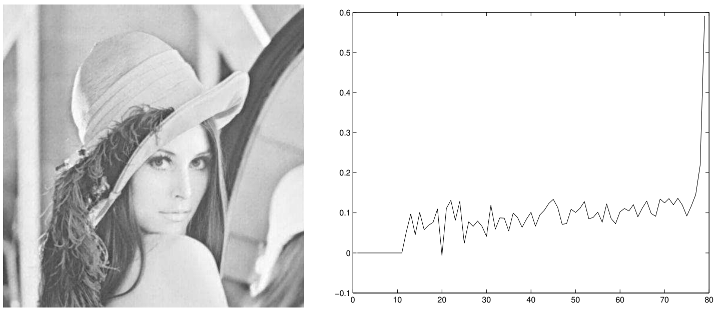

(a) (b)

Fig. 18. (a) Watermarked image after UnZign anti-watermarking system, (b) Normalized correlator output for several frequency sampling steps.

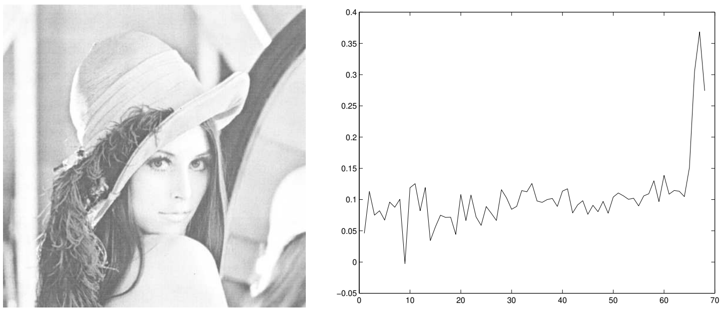

(a) (b)

Fig. 19. (a) Watermarked image after printing and re-scanning (b) Normalized correlator output for several frequency sampling steps.

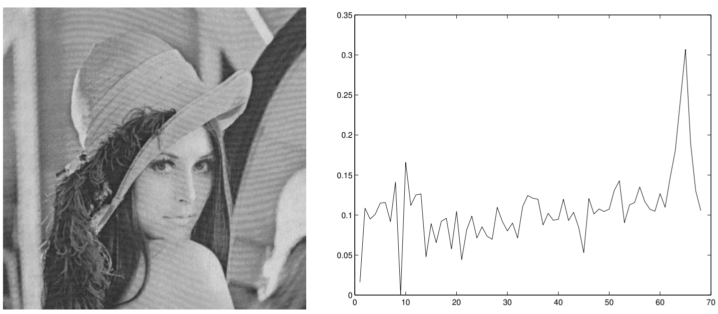

(a) (b)

Fig. 20. Watermarked image after printing, rotation and re-scanning (b) Normalized correlator output for several frequency sampling steps.

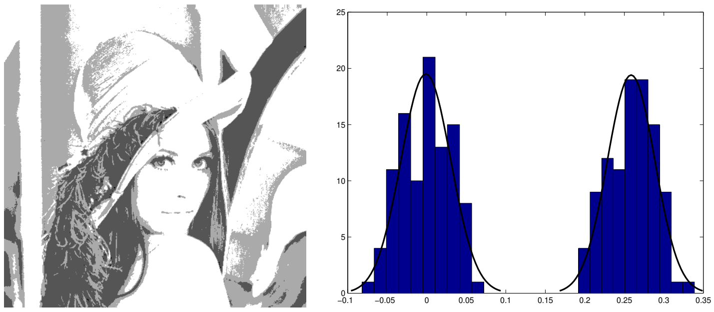

(a) (b)

Fig. 21. Watermarked image (quantization at 4 gray levels) (b) Empirical pdf of the normalized correlator output for 100 non-watermarked and watermarked grayscale quantized images (4 gray levels).

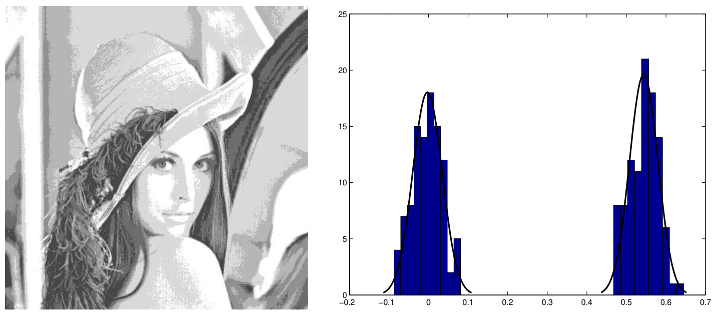

(a) (b)

Fig. 22. Watermarked image (quantization at 8 gray levels) (b) Empirical pdf of the normalized correlator output for 100 non-watermarked and watermarked grayscale quantized images (8 gray levels).

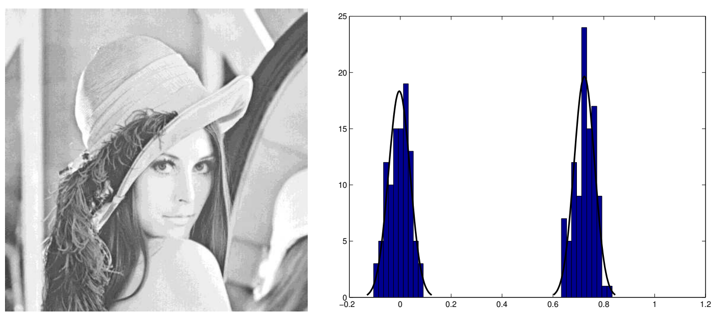

(a) (b)

Fig. 23. Watermarked image (quantization at 16 gray levels) (b) Empirical pdf of the normalized correlator output for 100 non-watermarked and watermarked color quantized images (16 gray levels).

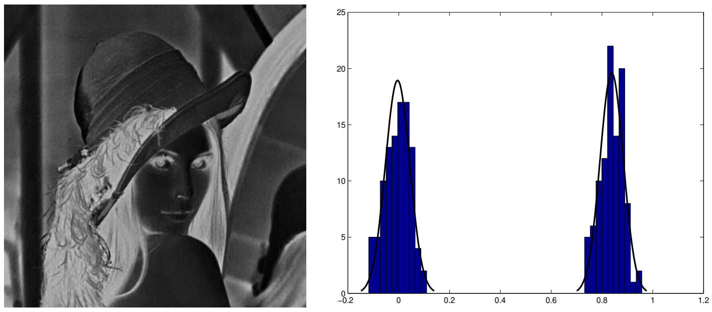

(a) (b)

Fig. 24. (a) Negative watermarked image. (b) Empirical pdf of the normalized correlator output for 100 non-watermarked and watermarked negative images.

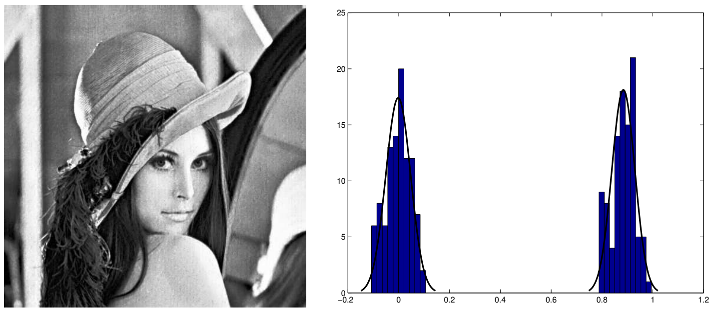

(a) (b)

Fig. 25. (a) Watermarked image after histogram equalization (b) Empirical pdf of the normalized correlator output for 100 non-watermarked and watermarked images after histogram equalization.

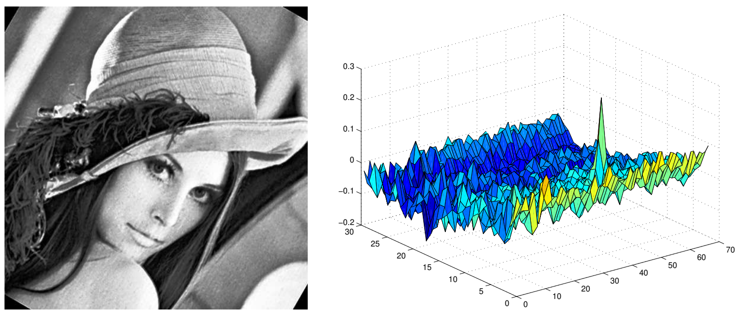

(a) (b)

Fig. 26. (a) Lenna undergone combined attacks (Jpeg compression to 14.22:1, rotation 30 degrees, cropping to 400×400, scaling to 512×512, histogram equalization) (b) Normalized detection output for several sampling steps and rotations.